

Supporting Information

Structural Analysis of Class I Lanthipeptides from *Pedobacter lusitanus* NL19 Reveals an Unusual Ring Pattern

Ian R. Bothwell^{1,§}, Tânia Caetano^{2,§}, Raymond Sarkisian¹, Sónia Mendo² and Wilfred A. van der Donk¹

¹ Howard Hughes Medical Institute and Department of Chemistry, University of Illinois at Urbana-Champaign, 600 South Mathews Ave, Urbana, IL 61822

² Molecular Biotechnology Laboratory, Department of Biology and CESAM, Campus de Santiago, University of Aveiro, 3810-189 Aveiro, Portugal

§ These authors contributed equally to this work

Supplemental Methods:

General methods. Reagents, buffer components and media were purchased from MilliporeSigma (Burlington, MA) or Fischer Scientific (Hampton, NH) unless otherwise noted. Oligonucleotides, enzymes, and buffers used for molecular biology were purchased from Integrated DNA Technologies Inc. (Coralville, IA) or New England Biolabs (Ipswich, MA). Plasmid isolation was conducted using QIAprep spin columns according to the manufacturer protocol (Qiagen, DE). Sequencing services were procured through ACGT Inc. (Wheeling, IL). *E. coli* NEB®5-alpha was used for cloning, selection and plasmid propagation, while *E. coli* BL21 Star (DE3) was used for peptide expression.

Plasmid construction. The plasmids constructed for this study are listed in Table S1 and their combined application for PedA15 production and purification is shown in Figure S1. The genes (*pedA15.1*, *pedA15.2*, *pedB15*, *pedC15* and *pedGluRS*) were amplified from total DNA purified from *P. lusitanus* NL19 with the NZYProof DNA polymerase (NZYTech), according to the manufacturer's recommendations, and using primers possessing the required restriction sites (Tables S1 and S2). *pedA15.1* and *pedA15.2* were cloned to encode His₆-PedA15.1 and His₆-PedA15.2 fusion peptides. The recipient vectors (pETDuet-1, pRSFDuet-1, pCDFDuet-1 and pACYCDuet-1) were purified with the NZYMiniprep kit (NZYTech). PCR products and vectors were digested with the appropriate FastDigest restriction enzymes (Thermo Fisher Scientific) (Table S1) for 1 h at 37 °C and separated by agarose gel electrophoresis. The digested PCR products and vectors were excised and purified from the gels with the NZYGelPure kit (NZYTech). Ligation was performed in a 20 µL reaction containing 50 ng of the vector, the insert at a molar ratio vector:insert of 1:3, 1 U of T4 DNA ligase (Thermo Fisher Scientific) and 1X T4 DNA ligase buffer. After 1 h, 5 µL of the ligation were used to transform *E. coli* NZY5α cells (NZYTech) and colonies were selected on LB agar plates supplemented with 50 µg/mL of ampicillin (pETDuet-1), 30 µg/mL of kanamycin (pRSFDuet-1), 34 µg/mL of chloramphenicol (pCDFDuet-1) or 50 µg/mL of streptomycin (pACYCDuet-1). Colonies with the desired plasmid were screened by colony-PCR with NZyTaq (NZYTech) and using the universal primers described for MCS-1 (pET Upstream Primer or pACYCDuetUP1 and DuetDOWN-1) or MCS-2 (DuetUP2 and T7 Term), following the manufacturer's recommendations. Positive colonies were selected for plasmid extraction and their MCS were sequenced (StabVida). pPedA15.1 and pPedA15.2 plasmids were used as vectors to construct pPedAC15.1 and pPedAC15.2 coexpression plasmids, respectively, according to the abovementioned protocol. The pPedGluRS/tRNA^{Glu} plasmid was obtained by Gibson assembly reaction containing the

PCR-linearized vector pCDFDuet-1 and two gBlocks (IDT) encoding the tRNA^{Glu} gene of *P. lusitanus* NL19. pCDFDuet-1 was linearized by PCR with the primers listed in Table S2 with the Phusion DNA polymerase (NEB), following the manufacturer's instructions, and purified with the QIAquick PCR purification kit (Qiagen). The two gBlocks were designed to encode the tRNA^{Glu} of *P. lusitanus* NL19 gene under the transcriptional control of a T7 promoter sequence and containing flanking regions compatible to the Gibson assembly procedure¹ (to allow 5'-end and 3'-end overlap). The reaction was performed in the following conditions: 50 ng of linearized pCDFDuet-1, 2 ng of each gBlock and 1X Gibson Master Mix, in a total volume of 20 μ L. The reaction was incubated at 50 °C for 1 h and used to transform *E. coli* 5-alpha cells (NEB). Positive clones were selected after overnight incubation at 37 °C in LB agar plates supplemented with 34 μ g/mL of chloramphenicol and screened by colony-PCR with the MCS-1 primers as above described. After plasmid extraction and confirmation of correct gBlock insertion and sequence by Sanger sequencing, pPedtRNA^{Glu} was used as cloning vector to express the *gluRS* gene of *P. lusitanus* NL19 in its MCS-2, as described above.

Site-directed mutagenesis of PedA15 peptides. PedA15.1 Ser-to-Ala variants were obtained by site directed mutagenesis of pPedA15.1 with the primers listed in Table S2. The reaction was performed according to the protocol described in reference² using the NZYProof DNA polymerase (NZYTech), followed by *DpnI* treatment (Thermo Fisher Scientific) and transformation of *E. coli* NZY5 α cells (NZYTech). Three Amp^R colonies were selected for plasmid purification and sequencing to confirm the presence of the target mutation in *pedA15.1*.

PedA15.1 Ser-to-Thr variants were generated by PCR using primers listed in Table S2. PCR reactions (50 μ L) contained 1x Phusion HF buffer, 200 μ M dNTPs, 0.5 μ M forward and reverse primer, 10 ng pPedA15.1 template, and 1 U Phusion® DNA

polymerase. Thermocycler conditions were as follows: initial denaturation, 98 °C, 30 s; 30 cycles of denaturation (98 °C, 10 s), annealing ($T_m + 5$ °C, 30 s), and extension (72 °C, 3 min); final extension, 72 °C, 4 min. Reactions were treated with *DpnI* to remove template and the product used to transform chemically competent *E. coli* NEB®5-alpha cells. Colonies were selected from LB agar containing ampicillin (Amp) at 37 °C overnight and propagated in liquid LB^{Amp} at 37 °C overnight prior to plasmid isolation and sequencing.

Heterologous expression of modified PedA and variants. Electrocompetent *E. coli* BL21 Star (DE3) were transformed with combinations of the plasmids prepared (see Supplemental Information) to coexpress enzymes as described in the Results section. Colonies were selected on LB agar plates containing the appropriate antibiotics listed for each plasmid. Single colonies were used to inoculate 5 mL overnight starter cultures in LB with the appropriate antibiotic. These cultures were then used to inoculate 2 L of TB expression cultures, which were incubated at 37 °C with shaking (200 rpm) until they reached an OD600 of approximately 0.8. Cultures were then cooled at 4 °C for 0.5 h prior to the addition of isopropyl β -D-1-thiogalactopyranoside (IPTG) to a final concentration of 0.5 mM. Cultures were placed into an 18 °C incubator and shaken overnight (200 rpm). Cells were harvested by centrifugation at 4,500 \times g for 15 min. The culture media was decanted and the cell paste stored at -80 °C prior to purification.

Purification of PedA15 peptides and proteolytic removal of leader peptides. Cell paste was suspended in 30 mL of lysis buffer (20 mM NaH₂PO₄, 500 mM NaCl, 0.5 mM imidazole, 20% glycerol, pH 7.5 at 25 °C) and lysed by sonication (40% amplitude, 4 s pulse, 9.9 s pause, 15 min). Crude lysate was centrifuged at 24,000 \times g for 30 min at 4 °C and the supernatant discarded. The pellet was washed with lysis buffer prior to suspension in approximately 20 mL of denaturing buffer (6 M guanidine hydrochloride, 20 mM NaH₂PO₄, 500 mM NaCl, 0.5 mM imidazole, pH 7.5 at 25 °C). The resolubilized

portion was cleared by centrifugation and the supernatant further clarified through a 0.45 μm syringe filter prior to loading onto Ni-nitrilotriacetic acid (NTA) resin equilibrated with denaturing buffer. After loading the filtered sample, the resin was washed with two column volumes (CV) each of denaturing buffer and washing buffer (4 M guanidine hydrochloride, 20 mM NaH_2PO_4 , 300 mM NaCl, 30 mM imidazole, pH 7.5 at 25 °C). The desired PedA peptide was eluted using 1–3 CV of LanA Elution Buffer (4 M guanidine hydrochloride, 20 mM Tris HCl, pH 7.5 at 25 °C, 100 mM NaCl, 1 M imidazole). Peptides eluted from NiNTA resin were desalted using Bond Elut C18 solid phase extraction cartridges (Agilent), washed with 0.1% TFA in water, and eluted in 60% acetonitrile in water supplemented with 0.1% TFA. Desalted peptide solutions were lyophilized prior to downstream proteolysis or HPLC purification.

Where noted in text, peptides were digested with LysN (Pierce™), trypsin (TPCK-treated; Worthington Biochemical), LahT(150), or pfu aminopeptidase I (Takara). The LahT(150) protease was purified according to previously reported procedures.³ LysN and trypsin reactions were conducted according to manufacturer instruction in 50 mM Tris HCl (pH 7.5) at a 1:100 (w/w) ratio of protease to substrate peptide in a 37 °C water bath overnight. Reactions containing LahT(150) were carried out in 50 mM Tris HCl (pH 7.5) at a 1:20 (w/w) ratio of protease to substrate at room temperature overnight. Reactions containing pfu aminopeptidase were conducted in 50 mM Tris HCl (pH 7.5) supplemented with 20 μM CoCl_2 at a 1:100 (w/w) ratio of protease to substrate incubated at 55 °C. Reactions were monitored by MALDI-MS after ZipTip cleanup and reaction times extended as needed. Upon completion, cleavage products were purified by HPLC or solid-phase extraction using Bond Elut C18 (Agilent) cartridges.

Matrix-assisted laser desorption/ionization time-of-flight mass spectrometry (MALDI-TOF MS) and MSMS analysis. Mass spectrometry analysis was

carried out at the University of Illinois at Urbana-Champaign School of Chemical Sciences Mass Spectrometry Laboratory using either an Autoflex speed LRF MALDI-TOF (Bruker) or an UltrafleXtreme MALDI-TOF/TOF MS instrument (Bruker). All samples were purified by HPLC or desalted using ZipTip C18 (Millipore) pipet tips prior to analysis. Samples were co-spotted (1:1 v:v) on MALDI plates with a 50 mg/mL solution of 2,5-dihydroxybenzoic acid (DHB, Sigma) in 60% acetonitrile:40% water as matrix. Data was analyzed using mMass software.⁴ MALDI-TOF MS was used for full-length peptides as this technique is well-suited for relatively high molecular weight peptides. However, mass accuracy at these m/z values is low for MALDI-TOF MS. Therefore, to verify correct structural assignment, full-length peptides were digested by proteases (see above) to obtain smaller peptides that were analyzed by high resolution ESI MS to obtain accurate m/z values. In addition, ESI was then used for tandem MS (MS/MS) experiments to also verify sequence identity. Generally the data by MALDI-TOF MS and ESI MS agreed with the exception of PedA15.1 for which a minor 6-fold dehydrated peptide was observed by ESI-MS but not MALDI-TOF MS.

LC-MS/MS was performed on a quadrupole/time-of-flight (Q/TOF) Synapt LC-MS (Waters) equipped with MassLynx software and a C18 UPLC column using a mobile phase of acetonitrile/water containing 0.1% formic acid (2-100% acetonitrile over 20 min; flow rate = 0.18 mL/min). Glu-1-fibrinopeptide B (Glu-Fib) was used for mass calibration prior to sample injection and data collection.

N-Ethylmaleimide (NEM) cysteine alkylation assay. The degree of cyclization of modified PedA15 peptides was determined through the alkylation of unreacted Cys thiols with NEM.⁵ Prior to alkylation, samples were treated with 10 mM tris(2-carboxyethyl)phosphine (TCEP) in reaction buffer (100 mM sodium citrate, 1 mM EDTA, pH 6) for 10 min to ensure complete reduction of free cysteines. NEM (100 mM freshly prepared stock solution in ethanol) was then added to a final concentration of 10 mM.

This reaction was allowed to proceed for 20 min before desalting using C18-ziptips and analysis by MALDI-TOF MS. Unmodified NisA or PedA precursor peptides were used as positive controls to ensure complete alkylation was achieved under these conditions.

Chiral gas chromatography – mass spectrometry. Purified PedA15 core peptides or variants (~0.5-1 mg) were dissolved in 3 mL of 6 N DCI in D₂O and sealed in a pressure tube. Each sample was heated to 110 °C in an oil bath for 24 h then cooled before solvent removal by rotary evaporation. In a separate flask, a solution of methanolic HCl was prepared by drop-wise addition of acetyl chloride (1.5 mL) to methanol (5 mL) in an ice-water bath. This solution (3 mL) was added to the hydrolysate residue and brought to 110 °C for 1 h under reflux. The reaction was allowed to cool prior to the removal of solvent by rotary evaporation. The resulting residue was then suspended in 3 mL of dichloromethane and cooled in an ice-water bath. Pentafluoropropionic anhydride (1 mL) was added to the reaction vessel, and the mixture heated to 110 °C for 1 h with reflux. The solution was cooled and the solvent removed under a gentle stream of nitrogen. The sample residue was then dissolved in 0.2 mL of methanol, centrifuged to remove any insoluble material, transferred to a clean vial, and stored at -20 °C prior to analysis. Gas chromatography–mass spectrometry (GC-MS) analysis was conducted on an Agilent HP 6890N instrument equipped with a CP-Chirasil-L-Val (Agilent) column (25 m x 0.25 mm x 0.12 µm). Samples in methanol (1–5 µL) were applied to the column via splitless injection (230 °C injector inlet temperature) with a helium flow at a rate of 1.7–2.0 mL/min. One of two temperature programs was used: (A) 5-min at 160 °C, followed by temperature increase of 3 °C min⁻¹ to 190 °C, and then held for 6 min; or (B) held at 80 °C for 5 min, then raised to 200 °C at a rate of 4 °C/min, and then held at 200 °C for an additional 3 min. Selected-ion monitoring (SIM) mode was used to detect characteristic mass fragments for derivatized lanthionine or methylanthionine (365 and 379 m/z, respectively). Stereochemical

determination for derivatized PedA15 samples was achieved through co-injection with pure synthetic standards prepared according to reported methods.⁶

NMR spectroscopy. Modified wild-type His₆-PedA15.1 was expressed and affinity purified from 4 L of *E. coli* culture grown as described above, yielding ~5 mg of semi-pure full-length modified peptide. This peptide was then digested with trypsin and purified by C18 RP-HPLC as described above to yield ~1 mg final product. Product purity was confirmed by NEM assay and MALDI-MS before proceeding to NMR analysis. Due to poor solubility in water, the modified core peptide was dissolved in dimethyl sulfoxide-d₆ (DMSO-d₆; Millipore-Sigma; 0.6 mL) and placed in an NMR tube. One dimensional ¹H NMR, and two-dimensional homonuclear ¹H-¹H-TOCSY (total correlation spectroscopy) and NOESY (nuclear Overhauser effect spectroscopy) spectra were acquired using a Varian INOVA 750 MHz spectrometer equipped with a 5 mm triple resonance (¹H-¹³C-¹⁵N) triaxial gradient probe with the use of VNMRJ 2.1B software and the BioPack suite of pulse sequences. The optimal temperature for analysis was determined to be 37 °C based on peak width. The data were processed using NMRPipe and subsequently analyzed in NMRViewJ. Chemical shift assignments are shown in Table S4.

Table S1. Plasmids constructed in this study. The primers used for each amplification are listed in Table S2.

Plasmid	Vector	MCS	Insert	Enzymes
pPedA15.1	pETDuet-1	MCS-1	<i>pedA15.1</i>	<i>Bam</i> HI, <i>Not</i> I
pPedA15.2	pETDuet-1	MCS-1	<i>pedA15.2</i>	<i>Bam</i> HI, <i>Not</i> I
pPedAC15.1	pPedA15.1	MCS-2	<i>pedC15</i>	<i>Nde</i> I, <i>Xho</i> I
pPedAC15.2	pRSFDuet-1	MCS-2	<i>pedC15</i>	<i>Nde</i> I, <i>Xho</i> I
pPedB15	pRSFDuet-1	MCS-1	<i>pedB15</i>	<i>Nco</i> I, <i>Not</i> I
pPedC15	pACYDuet-1	MCS-2	<i>pedC15</i>	<i>Nde</i> I, <i>Xho</i> I
pPedtRNA ^{Glu}	pCDFDuet-1	MCS-1	tRNA ^{Glu} NL19 x 2	N/A
pPedtRNA ^{Glu} /GluRS	pPedtRNA ^{Glu}	MCS-2	<i>gluRS</i> NL19	<i>Nde</i> I, <i>Xho</i> I

Table S2. Primers used in this study for site-directed mutagenesis.

Name	Sequence (5'->3')
pedA15.1_fw_BamHI	agtaggatccgatgaaaaagtaaagctaacca
pedA15.1_rv_NotI	cgatgCGGCCGCTtaattGCCAAAAattaattatcaag
pedA15.2_fw_BamHI	agtaggatccgatgaaaaagtaaagctaacca
pedA15.2_rv_NotI	cgatgCGGCCGCTtagtataatcttcccgtc
pedC15_fw_NdeI	agtacatatggaactattgaaaaatatgaaag
pedC15_rv_XhoI	cgatctcgagftaaggatccatgtaaattcat
pedB15_fw_NcoI	cgatccatgggcatgcaaaaagcaaaaattacc
pedB15_rv_NotI	cgatgCGGCCGCTtatgataatagtttaattggtg
pedGluRS_fw_NdeI	agtacatatggaagaaagtagtagtaag
pedGluRS_rv_XhoI	cgatctcgagftatccaaaagcagccagg
Gibson_pCDF_linear_fw	tcgtattgtacacggccg
Gibson_pCDF_linear_rv	tatagtgagtcgtattaatttcta
PedA151_S7T_F	ggataaattagagcccgtatacacgtcatattgtaggcattttaccacc
PedA151_S7T_R	ggtggtaaaaaatgcctacaatatgacgtgtataacgggctctaatttatcc
PedA151_S12T_F	ctgactgacaggataaattagtgccggtatacatgacatatt
PedA151_S12T_R	aatatgtcatgtataacgggcactaattatcctgtcagtcag
PedA151_S15T_F	gctgactgacaggftaaattagagcccgtatacatgac
PedA151_S15T_R	gtcatgtataacgggctctaatttaacctgtcagtcagc
PedA151_S18T_F	ctccggatcacatttcgccgtctgacaggataaattagag
PedA151_S18T_R	ctctaatttatcctgtcagacggcgaaatgtgatccggaag
Ped15_1_S7A_fw	aatgcctacaatatggcatgtataacgggctc
Ped15_1_S7A_rv	gagcccgtatacatgccatattgtaggcatt
Ped15_1_C8A_fw	taaattagagcccgtatagctgacatattgtaggcattttaccacc
Ped15_1_C8A_rv	gggtggtaaaaaatgcctacaatatgtcagctataacgggctctaattta
Ped15_1_T10A_fw	cctacaatatgtcatgtatagcgggctctaatttatcctg
Ped15_1_T10A_rv	caggataaattagagcccgtatacatgacatattgtagg
Ped15_1_S12A_fw	gtcatgtataacgggctctaatttatcctgtc
Ped15_1_S12A_rv	gacaggataaattagcggcgtatacatgac
Ped15_1_S15A_fw	cgggctctaatttagcctgtcagtcagc
Ped15_1_S15A_rv	gctgactgacaggctaaattagagcccg
Ped15_1_S26A_fw	tcagcgaaatgtgatccggaagaagctcttgataatttaattttgg
Ped15_1_S26A_rv	ccaaaaattaattatcaagagcttcttccggatcacatttcgctga

Table S3: Organisms tested for antimicrobial activity of PedA15.1 and 15.2 products, both individually and in combination.

Species	Media	Organism	Modified Core Peptides Tested*
<i>Micrococcus luteus</i> ATCC 4698	Nutrient	Gram positive Actinobacteria	PedA15.1 ^{LysN} and PedA15.2 ^{LahT150} PedA15.1 ^{LysN+AP} and PedA15.2 ^{LahT150+AP}
<i>E. coli</i> DH5 α	LB	Gram negative γ -proteobacterium	PedA15.1 ^{LysN} and PedA15.2 ^{LahT150} PedA15.1 ^{LysN+AP} and PedA15.2 ^{LahT150+AP}
<i>Bacillus subtilis</i> ATCC 6633	Nutrient	Gram positive Firmicute	PedA15.1 ^{LysN} and PedA15.2 ^{LahT150} PedA15.1 ^{LysN+AP} and PedA15.2 ^{LahT150+AP}
<i>Pseudomonas aeruginosa</i> strain K	Nutrient	Gram negative γ -proteobacterium	PedA15.1 ^{LysN} and PedA15.2 ^{LahT150} PedA15.1 ^{LysN+AP} and PedA15.2 ^{LahT150+AP}
<i>Saccharomyces cerevisiae</i>	YPD	yeast	PedA15.1 ^{LysN} and PedA15.2 ^{LahT150} PedA15.1 ^{LysN+AP} and PedA15.2 ^{LahT150+AP}
<i>Kluyveromyces lactis</i>	YPD	yeast	PedA15.2 ^{LahT150**}
<i>Aspergillus terreus</i>	YPD	fungus	PedA15.1 ^{LysN} and PedA15.2 ^{LahT150} PedA15.1 ^{LysN+AP} and PedA15.2 ^{LahT150+AP}
<i>Zygosaccharomyces rouxii</i>	YPD	yeast	PedA15.1 ^{LysN} and PedA15.2 ^{LahT150} PedA15.1 ^{LysN+AP} and PedA15.2 ^{LahT150+AP}
<i>Chryseobacterium gregarium</i> DSM 1909	Nutrient	Gram negative Bacteroidetes	PedA15.1 ^{Trypsin,†} and PedA15.2 ^{LahT150}
<i>Pedobacter alluvius</i> ATCC BAA-1554	Nutrient	Gram negative Bacteroidetes	PedA15.1 ^{Trypsin,†} and PedA15.2 ^{LahT150}

*Superscript denotes proteases used to generate the core peptide fragments used during bioactivity screening. Following LysN or LahT150 digestion, peptides were first partially purified by C18 SPE and tested prior to a second digestion with Pfu aminopeptidase ("AP", Takara Bio) and subsequent testing.

** Insufficient material for testing PedA15.1.

† At the time that these experiments were done, endoproteinase LysN was no longer commercially available and trypsin was used to remove the leader peptide, which removes one more Lys residue.

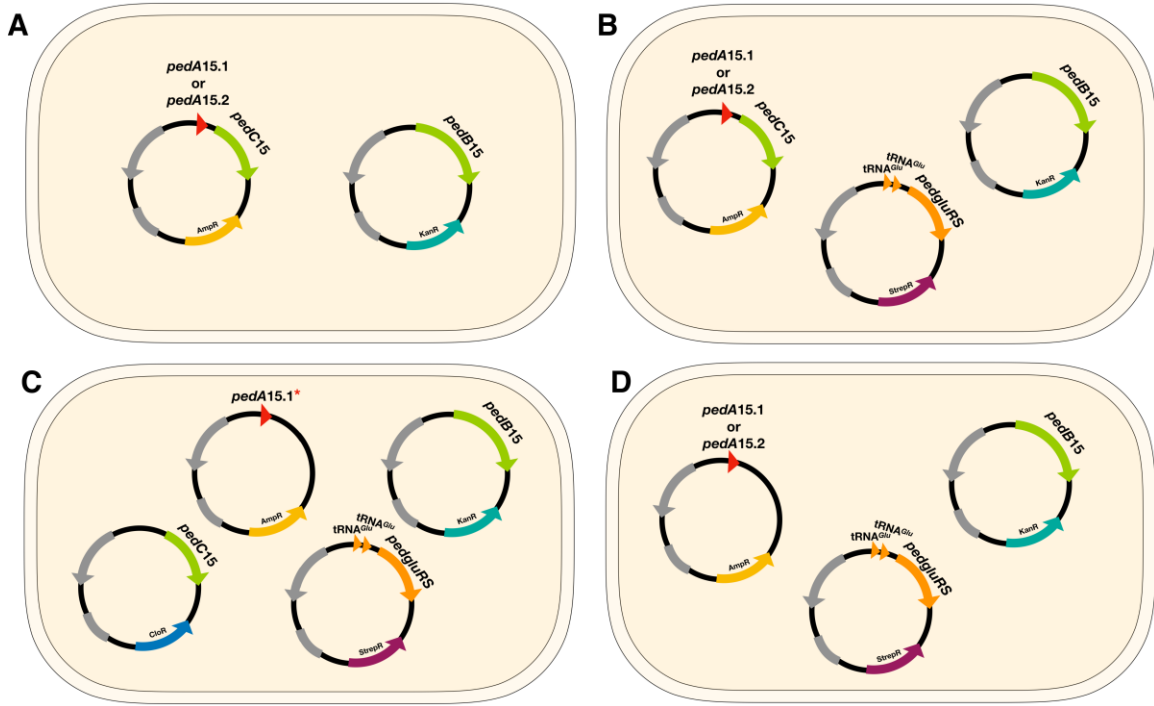


Figure S1: Schematic representation of the *ped15* expression systems in *E. coli* BL21(DE3) used in this study. The PedA15.1 and PedA15.2 peptides produced with the first system (A), which did not include the *tRNA^{Glu}* and *gluRS* genes of *P. lusitanus* NL19, were not dehydrated by PedB15. However, in the presence of these two genes (B), PedB15 was able to dehydrate both PedA15 peptides. Finally, to ease the production of PedA15.1 variants a third system was developed (C). In the last system, *pedA15.1* was expressed in an independent vector, which allows its use in site-directed mutagenesis, followed by transformation of *E. coli* BL21(DE3) competent cells harboring three plasmids that express all the other genetic determinants required for PedA15.1 modification. Panel D corresponds to the *E. coli* expression system that allowed the purification of PedA15 peptides without modification by PedC15.

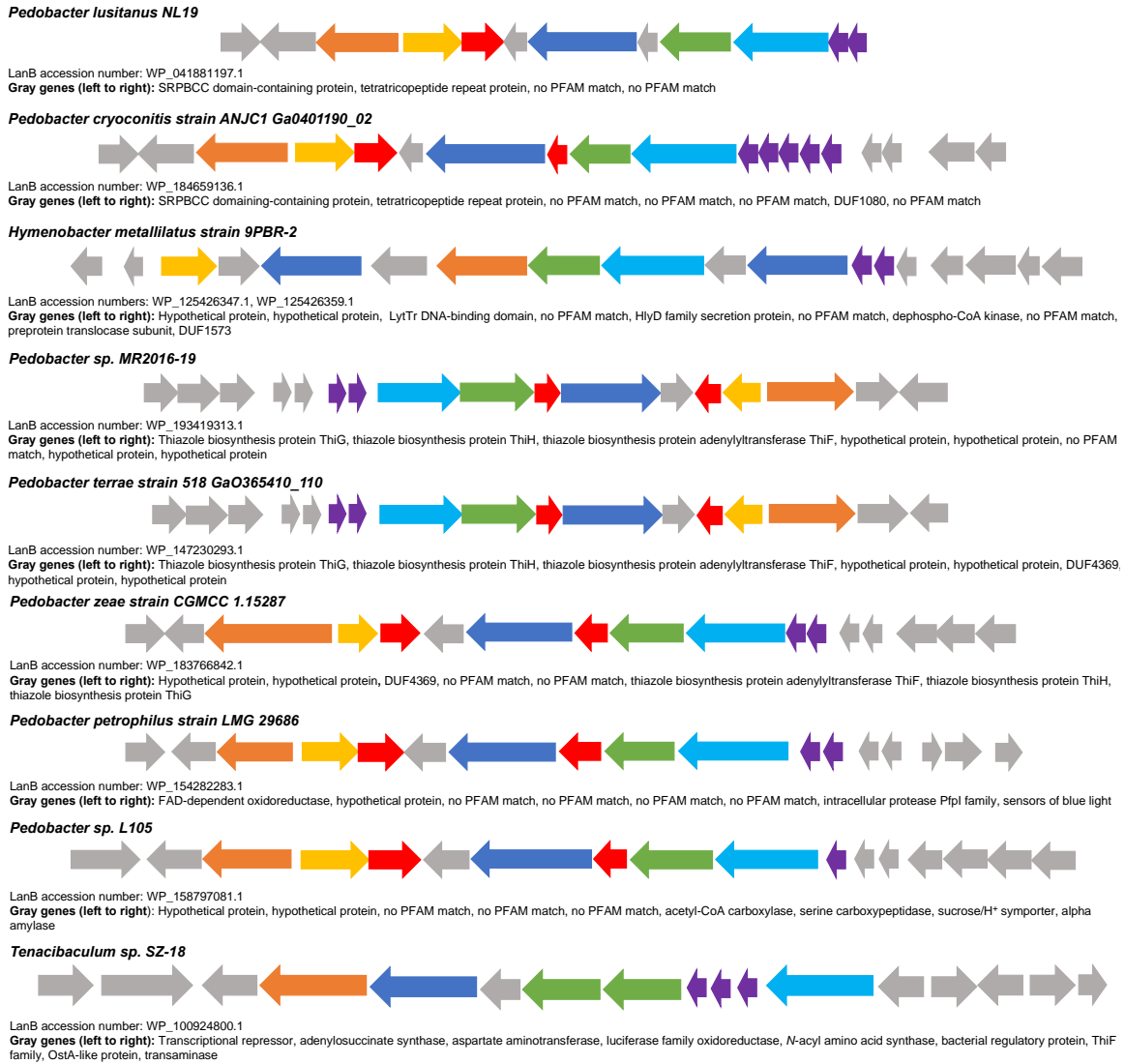
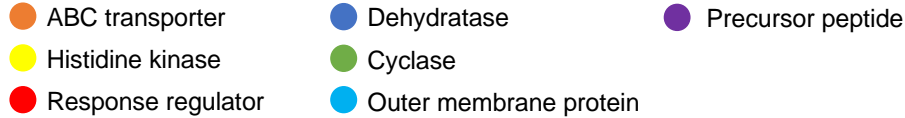


Figure S2. Gene neighborhood of BGCs resembling the cluster in *P. lusitanus*. The genes located up and downstream of the colored core genes depicted in Figure 1B are not conserved across the BGCs suggesting that they are not part of a conserved biosynthetic pathway. The predicted function of the grey genes on both ends of the BGC are shown below each cluster. The LanB accession number is given for each BGC for reference. For sequences of the putative precursor peptides, see Figure S13. The BGC in *P. lusitanus* NL19 is at the end of a contig and hence no information is available regarding the genes that flank the precursor peptide genes. The last partial ORF on the contig appears to encode another PedA ortholog.

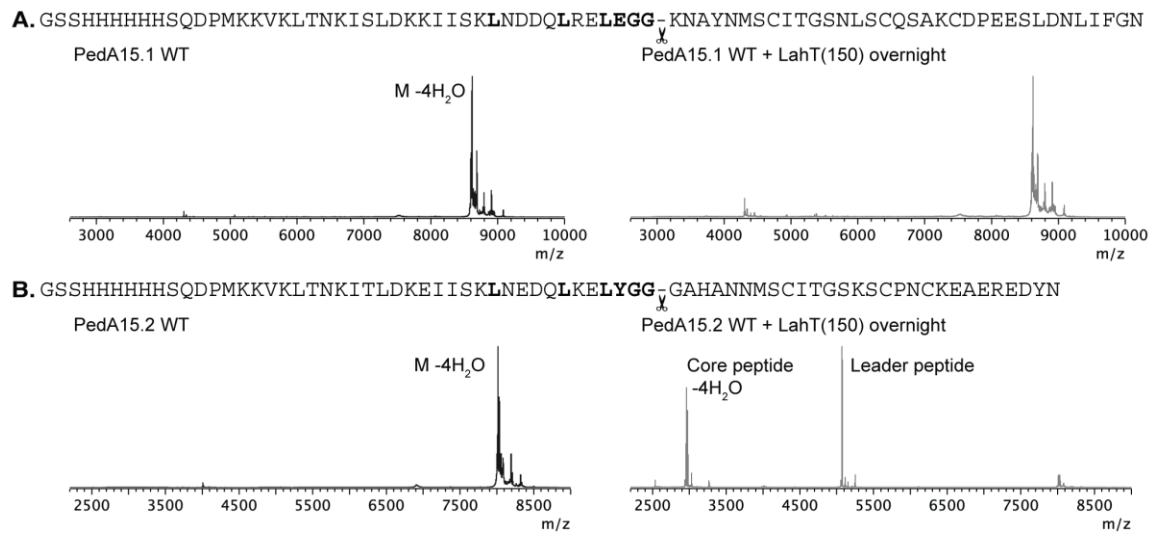


Figure S3: Susceptibility of PedA15 peptides towards LahT150 for leader peptide removal. (A) His₆-tagged wild-type Ped15B/C-modified PedA15.1 before (left, black) and after (right, grey) overnight incubation with LahT150. The full-length peptide was modified (4x dehydrated, [M+H]⁺ avg., m/z 8616.592 calc.; 8616.740 obs.), however, no proteolysis by LahT150 could be observed after overnight incubation. (B) His₆-tagged Ped15B/C-modified PedA15.2 before (left, black) and after (right, grey) overnight incubation with LahT150. Proteolysis of full-length PedA15.2 was apparent by the appearance of mass fragments consistent with 4x dehydrated core peptide ([M]⁺ avg., m/z 2958.2 calc.; 2958.0 obs.) and the leader peptide ([M]⁺ avg., m/z 5072.7 calc.; 5072.4 obs.).

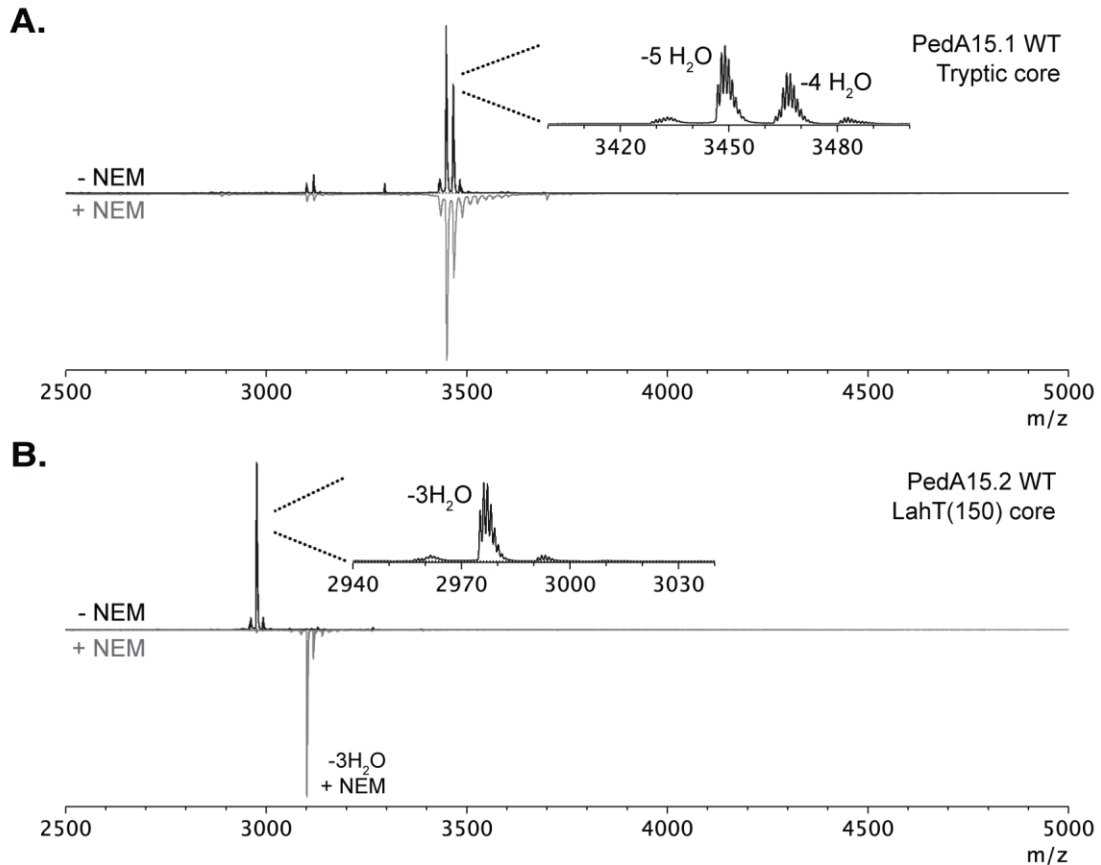


Figure S4: MALDI-TOF MS analysis of HPLC-purified PedA15.1 and PedA15.2 core peptide fragments. PedA peptides were coexpressed with PedB15, PedC15, and *P. lusitanus* tRNA^{Glu}/GluRS. (A) PedA15.1 tryptic core peptide was purified by HPLC prior to MALDI-TOF MS analysis before (black) and after (grey) treatment with NEM. Purified product contained fully cyclized product and contained mainly 5x dehydrated ([M] avg., m/z 3449.8 calc.; 3449.4 obs.) product, although some 4x dehydrated ([M+H] avg., m/z 3466.5 calc.; 3466.6 obs.) peptide was also present and could not be separated by HPLC. (B) PedA15.2 leader peptide was removed by digestion with LahT150 and the 3x dehydrated core peptide purified by HPLC prior to MALDI-TOF MS analysis before (top) and after NEM alkylation (bottom). Thus, unlike four times dehydrated PedA15.2 (Fig. S3), 3x dehydrated ([M] avg. m/z 2974.2 calc.; 2974.4 obs.) PedA15.2 has a free Cys that has not cyclized and could be separated by HPLC.

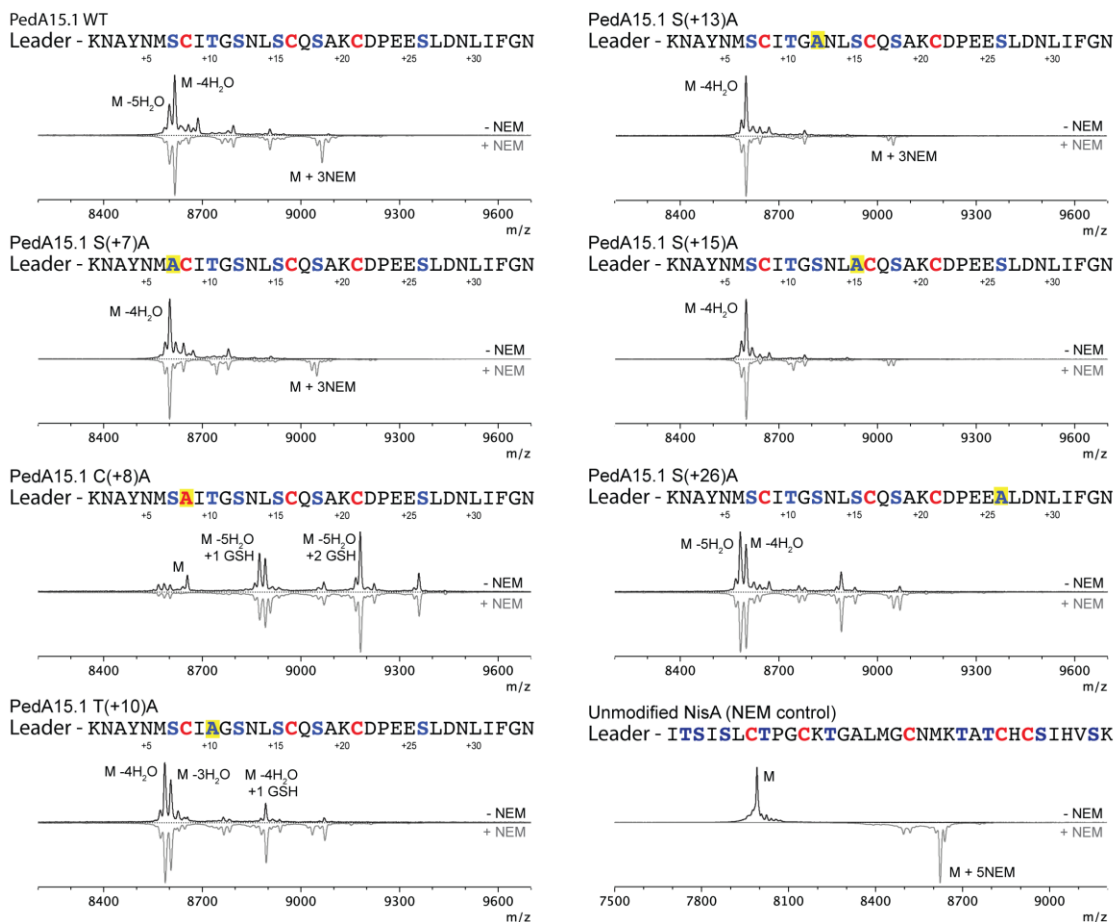


Figure S5: Ser-to-Ala PedA15.1 variants co-expressed with Ped15B/C. Peptides were analyzed by MALDI-TOF MS prior to (top; black) and after (bottom; grey) NEM alkylation. The S7A, S12A, and S15A variants (mutation highlighted in yellow) are all dehydrated four times suggesting the Ser residues at these positions are dehydrated in the 5-times dehydrated wild-type product. The lack of NEM alkylation observed for all three peptides suggests that all Cys residues are cyclized, which is only possible if non-natural Lan/MeLan rings are formed. Such observations have been reported previously for lanthipeptide variants and illustrates the peril of ring assignments based on alanine scanning mutations.⁷ We therefore commenced with NMR experiments to determine the ring pattern as described in the main text. WT, wild-type; NEM, *N*-ethylmaleimide. Right bottom: NisA precursor peptide was included for analysis to ensure complete alkylation by NEM was taking place under the reaction conditions.

PedA15.1 Trypsin: NAYNM**SCITGSNLS**SCQ**SAKCDPEESLDNLI**FGN

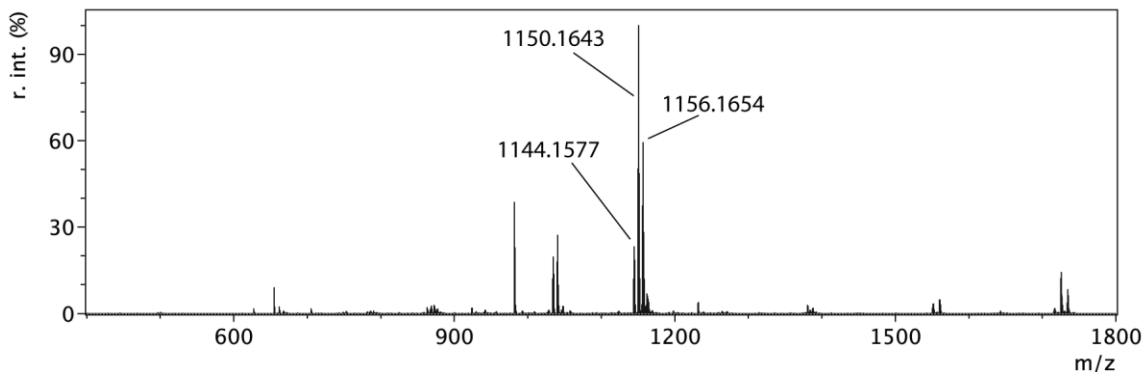


Figure S6: LC-MS analysis (ESI) of 6-, 5-, and 4-fold dehydrated PedA15.1 after trypsin digestion. $[M+3H]^{3+}$ is depicted for the various dehydration states. The peak values in the figure are the monoisotopic masses, which are given below: observed and calculated m/z: PedA15.1 – 6 H₂O (m/z 1144.1486 calc.; 1144.1577 obs.), PedA15.1 – 5 H₂O (m/z 1150.1536 calc.; 1150.1643 obs.), PedA15.1 – 4 H₂O (m/z 1156.1587 calc.; 1156.1654 obs.). The minor 6-fold dehydrated peptide was not observed by MALDI-TOF MS. The additional dehydration likely involves Ser26 because that is the only additional Ser/Thr in the peptide.

PedA15.2 LahT150: GAHAN**MS**C**ITG**S**KS**C**P**N**C**KEA**ER**D**Y**N

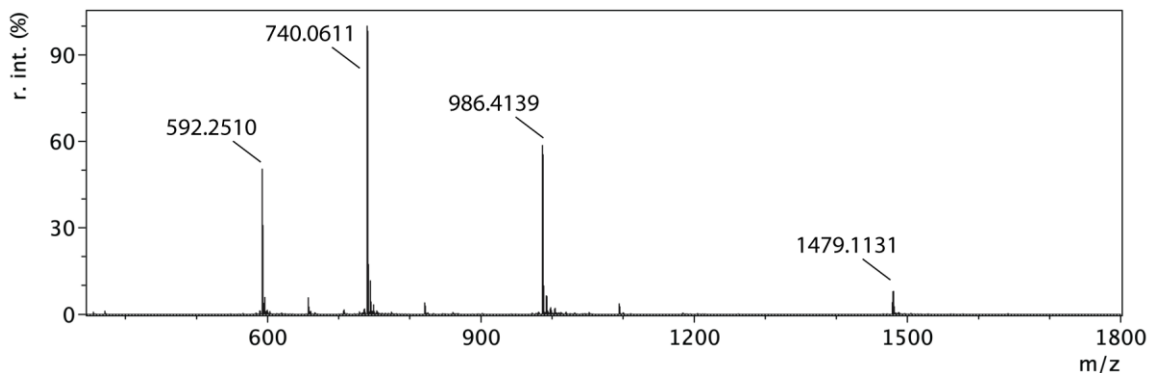
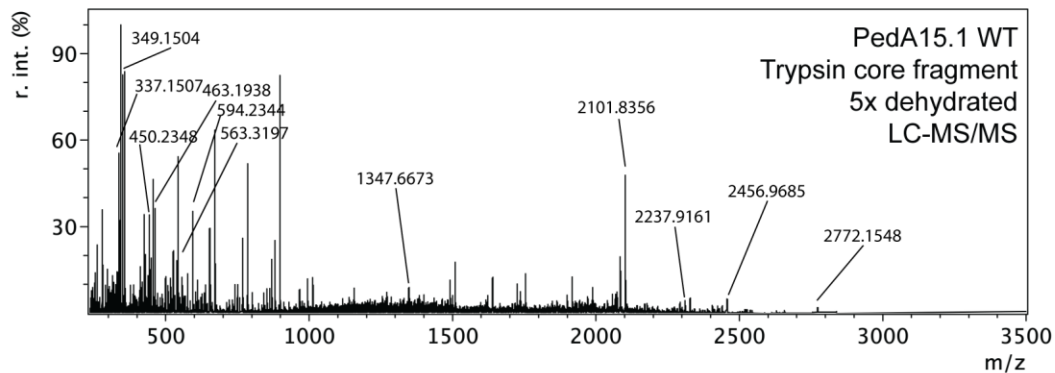


Figure S7: LC-MS analysis (ESI) of 4-fold dehydrated PedA15.2 after LahT150 digestion. $[M+5H]^{5+}$, $[M+4H]^{4+}$, $[M+3H]^{3+}$, and $[M+2H]^{2+}$ were observed. The peak values in the figure are monoisotopic masses, which are given below. m/z: PedA15.2 – 4 H₂O, $[M+H]^{5+}$ (m/z 592.2456 calc.; 592.2510 obs.), PedA15.2 – 4 H₂O, $[M+4H]^{4+}$ (m/z 740.0552 calc.; 740.0611 obs.), PedA15.2 – 4 H₂O, $[M+3H]^{3+}$ (m/z 986.4046 calc.; 986.4139 obs.), PedA15.2 – 4 H₂O, $[M+2H]^{2+}$ (m/z 1479.1033 calc.; 1479.1131 obs.).

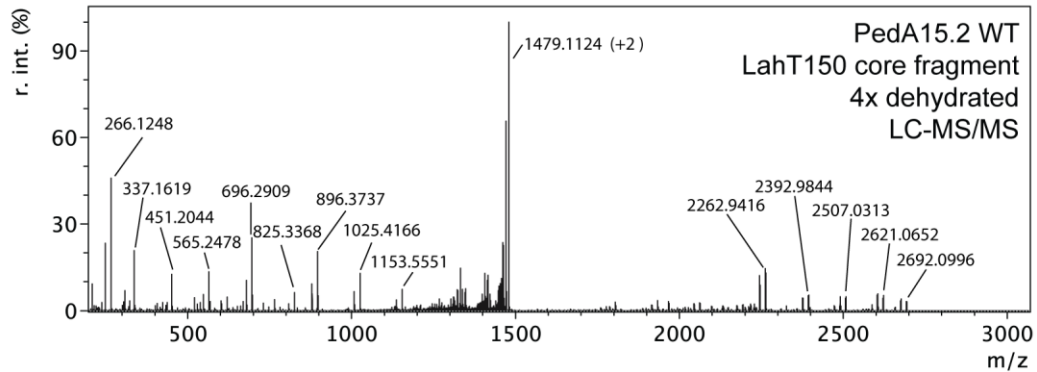
PedA15.1 Trypsin: NAYNM**S**C**I**T**G**SNL**S**C**Q**S**A**K**C**D**P**E**E**S**L**D**N**L**I**F**G**N
 b3 b4 b5 y12 y5 y4 y3
 b21 b23 b24 b27



b ⁺ ions				y ⁺ ions		
obs.	calc.	#	AA	#	calc.	obs.
	115.0502	1	N	33		
	186.0873	2	A	32	3334.4036	
349.1504	349.1506	3	Y	31	3263.3665	
463.1938	463.1936	4	N	30	3100.3032	
594.2344	594.2341	5	M	29	2986.2602	
	663.2508	6	S	28	2855.2198	
	766.2600	7	C	27	2786.2030	
	879.3441	8	I	26	2683.1938	
	962.3765	9	T	25	2570.1098	
	1019.3979	10	G	24	2487.0774	
	1088.4147	11	S	23	2430.0559	
	1202.4576	12	N	22	2361.0391	
	1315.5417	13	L	21	2246.9962	
	1384.5584	14	S	20	2133.9122	
	1487.5676	15	C	19	2064.8954	
	1615.6262	16	Q	18	1961.8862	
	1684.6429	17	S	17	1833.8276	
	1755.6800	18	A	16	1764.8109	
	1883.7750	19	K	15	1693.7738	
	1986.7842	20	C	14	1565.6788	
2101.8356	2101.8111	21	D	13	1462.6696	
	2198.8639	22	P	12	1347.6427	1347.6673
2237.9161	2327.9065	23	E	11	1250.5899	
2456.9685	2456.9491	24	E	10	1121.5473	
	2543.9811	25	S	9	992.5047	
	2657.0652	26	L	8	905.4727	
2772.1548	2772.0921	27	D	7	792.3886	
	2886.1350	28	N	6	677.3617	
	2999.2191	29	L	5	563.3188	563.3197
	3112.3032	30	I	4	450.2347	450.2348
	3259.3716	31	F	3	337.1506	337.1507
	3316.3930	32	G	2	190.0822	
		33	N	1	133.0608	

Figure S8: LC-MS/MS analysis (ESI) of 5x dehydrated PedA15.1 core peptide with observed b- and y-ions labeled. The most C-terminal serine evades dehydration in this peptide. A lack of fragmentation within the central part of the peptide sequence is consistent with formation of overlapping lanthionines.

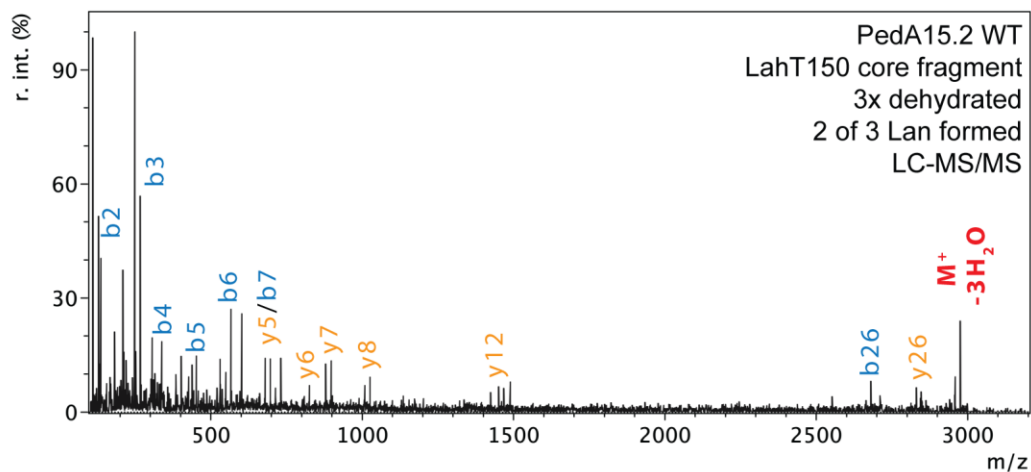
PedA15.2 LahT150: GAHANNM**SC**ITG**SK**SCPN**C**KEAEREDYN
 y25y24y23y22 y8 y7 y6 y5
 b3 b4 b5 b6 b7



b ⁺ ions				y ⁺ ions		
obs.	calc.	#	AA	#	calc.	obs.
	58.0287	1	G	28		
	129.0659	2	A	27	2900.1779	
	266.1248	3	H	26	2829.1408	
	337.1619	4	A	25	2692.0818	2692.0996
	451.2044	5	N	24	2621.0447	2621.0652
	565.2478	6	N	23	2507.0018	2507.0313
	696.2909	7	M	22	2392.9589	2392.9844
Lanthionine Region	765.3050	8	Dha	21	2261.9184	
	868.3142	9	C	20	2192.9016	
	981.3982	10	I	19	2089.8925	
	1064.4306	11	Dhb	18	1976.8084	
	1121.4521	12	G	17	1893.7760	
	1190.4688	13	Dha	16	1836.7545	
	1318.5638	14	K	15	1767.7378	
	1387.5805	15	Dha	14	1639.6428	
	1490.5897	16	C	13	1570.6261	
	1587.6425	17	P	12	1467.6169	
	1701.6854	18	N	11	1370.5641	
	1804.6946	19	C	10	1256.5212	
		1932.7896	20	K	9	1153.5120
	2061.8322	21	E	8	1025.4170	1025.4166
	2132.8693	22	A	7	896.3745	896.3737
	2261.9119	23	E	6	825.3373	825.3368
	2418.0130	24	R	5	696.2947	696.2909
	2547.0556	25	E	4	540.1936	
	2662.0825	26	D	3	411.1510	
	2825.1458	27	Y	2	296.1241	
		28	N	1	133.0608	

Figure S9: LC-MS/MS analysis of 4x dehydrated PedA15.2 core peptide with observed b- and y-ions labeled. A lack of fragmentation within the central part of the peptide sequence is consistent with lanthionine ring formation.

PedA15.2 LahT150: GAHANM**S**CI**T**GS**K**S**C**PN**C**KEAEREDYN
 b2b3b4b5b6b7 y26 y12 y8y7y6y5 b26



b ⁺ ions				y ⁺ ions			
obs.	calc.	#	AA	#	calc.	obs.	
	58.0287	1	G	28	2975.2147	2975.2698	
129.1047	129.0659	2	A	27	2918.1931		
266.1297	266.1248	3	H	26	2847.1560	2846.1252	
337.1659	337.1619	4	A	25	2710.0971		
451.2054	451.2048	5	N	24	2639.0600		
565.2441	565.2477	6	N	23	2525.0171		
696.2845	696.2882	7	M	22	2410.9742		
Lanthionine Region	765.3050	8	Dha	21	2279.9337		
	868.3142	9	C	20	2210.9169		
	981.3982	10	I	19	2107.9077		
	1064.4306	11	Dhb	18	1994.8237		
	1121.4521	12	G	17	1911.7913		
	1208.4841	13	S	16	1854.7698		
	1336.5791	14	K	15	1767.7378		
	1405.5958	15	Dha	14	1639.6428		
1508.6050	16	C	13	1570.6261			
	1605.6578	17	P	12	1467.6169	1467.6117	
	1719.7007	18	N	11	1370.5641		
	1822.7099	19	C	10	1256.5212		
	1950.8048	20	K	9	1153.5120		
	2079.8474	21	E	8	1025.4170	1025.4194	
	2150.8845	22	A	7	896.3745	896.3729	
	2279.9271	23	E	6	825.3373	825.3412	
	2436.0283	24	R	5	696.2947	696.2845	
	2565.0708	25	E	4	540.1936		
2680.1108	2680.0978	26	D	3	411.1510		
	2843.1611	27	Y	2	296.1241		
	2957.2041	28	N	1	133.0608		

Figure S10: LC-MS/MS analysis of 3x dehydrated PedA15.2 core peptide with observed b- and y-ions labeled. Presence of the y12 ion suggests that Cys19 evades cyclization in this intermediate, possibly a consequence of incomplete dehydration for the 3x-dehydrated species.

Table S4. Chemical shift assignments for 4-fold dehydrated PedA15.1 core peptide.

Residue*	HN	H α	H β	Others
Asn (2)				
Ala (3)	8.454	4.257	1.191	
Tyr (4)	7.974	4.381	2.918, 2.701	6.640 3H, 5H; 7.016 2H, 6H
Asn (5)	8.062	4.543	2.607, 2.461	6.877, 7.381 γ NH ₂
Met (6)	7.920	4.397	1.970	2.409 γ CH ₂
Ser (Lan; 7)	8.295	4.432	2.965	
Cys (Lan; 8)	7.639	4.681	3.0831, 2.882	
Ile (9)	8.035	4.156	1.826	1.532-1.194 γ CH ₂ ; 0.942 γ CH ₃ ; 0.874 δ CH ₃
Thr (Dhb10)**	9.355	-	6.423	1.672 γ CH ₃
Gly (11)	8.057	3.805, 3.642		
Ser (12)***	7.288	4.291	3.657, 3.712	
Asn (13)	8.440	4.477	2.549	6.844, 7.327 γ NH ₂
Leu (14)	7.795	4.230	1.593	1.496 γ CH; 0.870, 0.810 δ CH ₃
Ser (Lan; 15)	7.504	4.463	2.901, 3.022	
Cys (Lan; 16)	8.057	4.121	3.032, 2.904	
Gln (17)	7.970	4.098	1.855	2.129 γ CH ₂ ; 6.728, 7.214 γ NH ₂
Ser (Lan; 18)	8.328	4.824	2.869, 2.974	
Ala (19)	8.135	3.976	1.373	
Lys (20)	7.623	4.391	2.023, 1.441	1.305 γ CH ₂ ; 1.569 δ CH ₂ ; 2.779 ϵ CH ₂
Cys (Lan; 21)	6.885	4.021	3.295, 2.709	
Asp (22)	8.380	4.753	2.696, 2.402	
Pro (23)	-	4.310	2.043, 1.908	1.876 γ CH ₂ ; 3.645 δ CH ₂
Glu (24)	7.896	4.163	1.932, 1.793	2.257 γ CH ₂
Glu (25)	7.696	4.286	1.757, 1.935	2.226 γ CH ₂
Ser (26)	7.817	4.327	3.599	
Leu (27)	7.957	4.268	1.490	1.625 γ CH; 0.829, 0.870 δ CH ₃
Asp (28)	8.055	4.508	2.681, 2.500	
Asn (29)	7.879	4.504	2.549, 2.467	
Leu (30)	7.716	4.228	1.466	1.599 γ CH; 0.807, 0.863 δ CH ₃
Ile (31)	7.536	4.061	1.668	1.302-1.052 γ CH ₂ ; 0.667 γ CH ₃ ; 0.749 δ CH ₃
Phe (32)	7.814	4.533	3.051, 2.813	7.230 3H, 5H; 7.158 4H; 6.706 2H, 6H
Gly (33)	8.005	3.733		
Asn (34)	7.974	4.547	2.561, 2.479	7.334, 6.9057 γ NH ₂

* Residues are numbered according to their position relative to the Gly-Gly leader peptide proteolytic site. Lys1 was removed through the use of trypsin for leader peptide removal from the core peptide in this experiment.

** a faint set of signals indicative of Dhb at this residue was observed at 9.040 (NH), 6.232 (vinylic CH) and 1.680 (CH₃) ppm. We attribute these signals to the presence of a 5-fold dehydrated peptide that is additionally dehydrated at Ser26.

*** Due to the presence of both 4x and 5x dehydrated products, signals for both Ser12 and Dha12 are visible in the spectra. Ser12 chemical shifts are shown in the table above, whereas the presence of Dha12 is clearly evident by geminal vinylic signals at 5.550 and 5.226.

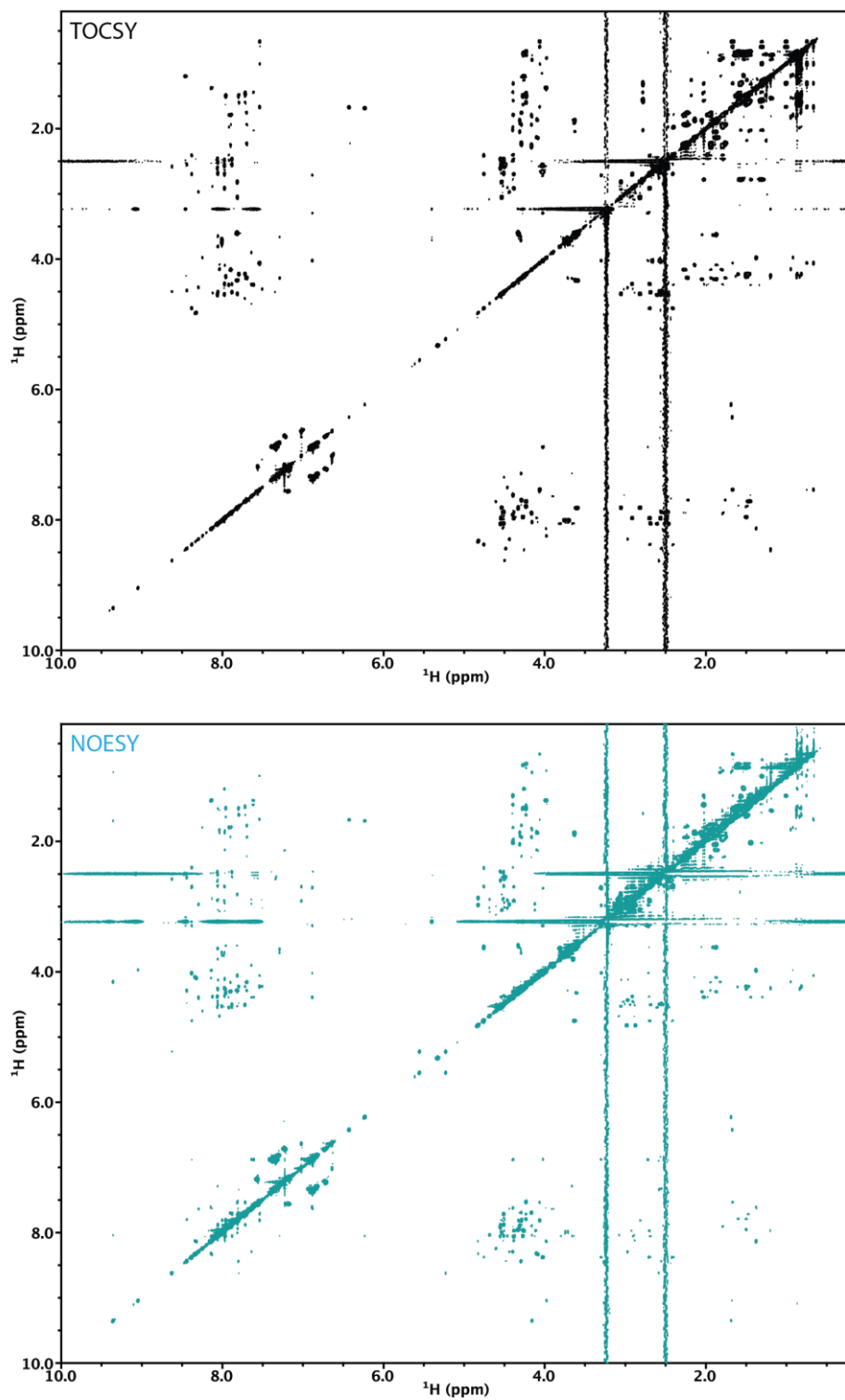


Figure S11: PedA15.1 core peptide TOCSY and NOESY spectra used for structural assignment and topology determination.

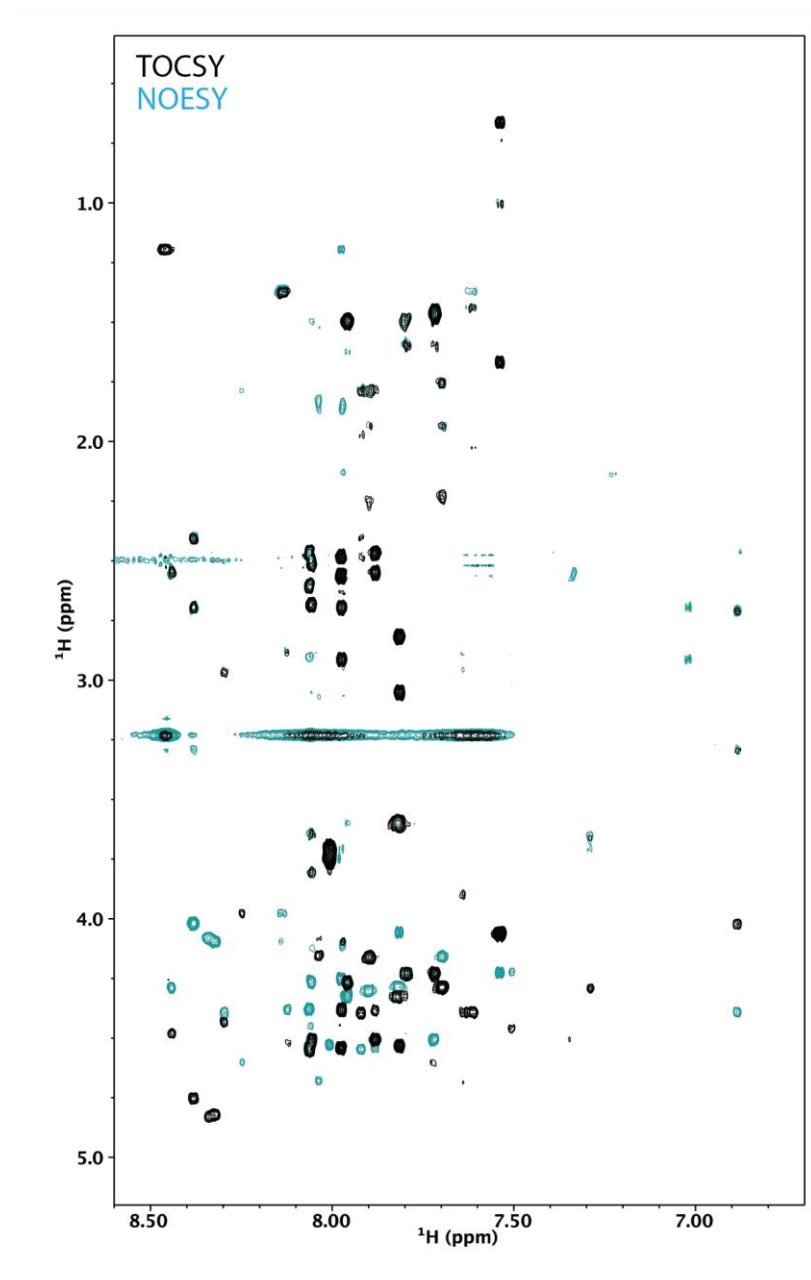


Figure S12: Zoomed overlay of TOCSY and NOESY spectra in the fingerprint region. Identified TOCSY spin-systems were correlated in-sequence through cross-reference to the NOESY spectra.

	-12 -7 -1	
WP_041881204.1	MKKVKLTNKITLDKEII SKLNEDQLKELYGG	GAHANNMSCITGSKSCPNCKEAEREDYN---
WP_200890725.1	----NLSDKVQLDKEIISKLTQDQLSELEGG	--AKQGLSCITGDNCKGVQQPEVDASL---
WP_183879665.1	MKKVNLNKNITLDKEIISKLNDDQLNELEGG	-KAAGSMSCITLSNQSCVSNANCEEAAQQRLSL
WP_183879663.1	MKKVNLSDRVQLDKEIISKLSEDQLSELEGG	--AKQGLSCITGENSCKTVQSQDAADEAL--
WP_183879661.1	MKKVNLSDKVQLDKEIISKLSEDQLSELEGG	--AKQGLSCITGDNCKTVKQDAVDDAL--
WP_183879658.1	MKKVNLSEKVQLDKEIISKLTEDQLSELEGG	--AKQGLSCVTGNNSCKTVQPQEAEEAL--
WP_183879656.1	MKKVNLSEKVQLDKEIISKLSDDQLKELEGG	-SGKGLSCIGGKDCVSKVSPQEEELS---
WP_184623960.1	MKKVNLSEKVQLDKEIISKLNDDQLKELEGG	-AAEKELSCIGGNNSCASKTIEAES-----
WP_184623961.1	MKKVNLSEKVQLDKEIISKLNDDQLKELEGG	-AAERELSCIGGNNSCASKTIEAES-----
WP_184623962.1	MKKVNLSEKVQLDKEIISKLSDDQLKELEGG	-AAEREVSCVTGNNSCATKTIEAES-----
WP_184623963.1	MKKVNLSDRIQLDREIISKLNDDQLKELEGG	--QTTSLSCITGTTSCVYQVPDES-----
WP_184623964.1	MKKVNLSEKVQLDKEIISKLNDDQLKELEGG	-AAEREVSCITGNNSCAAQELSES-----
WP_185816813.1	MKKVTLADQLELSKEIVANLTDEQLQEIEGG	-AAAAGISCITGSGSCSKTQAEAEELSE----
WP_185816814.1	MKKVSLADQLELSKEVIASLNDEQLQEIEGG	-AAAAGISCITGSGSCSKTQAEAEELSE----
WP_193419308.1	MKKVNLSDKVQLDKEIISKLSEDQLKEIEGG	--NAAEFSCVSD--SCKNNTKASLEEEELGG-
WP_193419309.1	MKKVKLLNKAQLEKEIISELSEDQLKEVQGG	--NAIEFSCWAD--SCKGPVKEDQDITLGD--
WP_168202517.1	MKKVNLSEKVQLDKEIISKLSEDQLKEIEGG	--NAAELSCWSD--SCKNNTKASLEEEFEGG-
WP_168202518.1	MKKVKLSNKVQLEKEIISELSEDQLKEVEGG	--NAIEFSCWAD--SCNRPIKGEQDAISD--
WP_183766852.1	MKKVNLSEKVQLDKEIISKLSEDQLKEIEGG	--NAAELSCWSD--SCKNNTKASVEEEIIGG-
WP_154282287.1	MKKVKLSNKVQLEKEIISELSEEQLKEVQGG	--NATEFSCWLD--SCKGPMKEQDAIDD---
WP_158797085.1	MKKVNLSEKVQLDKEIISKLTTEEQLKQIEGG	--NAAELSCWSD--SCKNNSVEEAN-----
WP_157811775.1	MNKIKLTKGLQINKEVSKLQEDQMADVKGG	---KAALSCLWK--SCNGSKEDKLEA-----
WP_157811776.1	MKKIKLTKGLQINKEAVSKLQEDQMTEVKGG	---KAALSCLWK--SCNSSSEESIEA-----
WP_157811777.1	MKKIKLTKGLKINKEAISKLQEDQMTEVKGG	---KAALSCLWD--SCNGSSEEKLEL-----

Figure S13: Sequence alignment of lanthipeptide precursor peptides encoded in genomes of various Bacteroidetes. Peptide sequences were obtained by performing a BLAST analysis⁸ with PedA15.1 as query followed by RODEO analysis⁹ to assure nearby LanB, and LanC enzymes. Peptides containing a double-glycine motif at the end of the putative leader peptide, as well as a hydrophobic residue at -7 and -12 positions (grey) that are known recognition positions for LanT proteases were selected for alignment. All peptides contain a SCX_nSC motif ($n = 3-6$; yellow). Peptide sequences from different biosynthetic gene clusters are separated with an empty line.

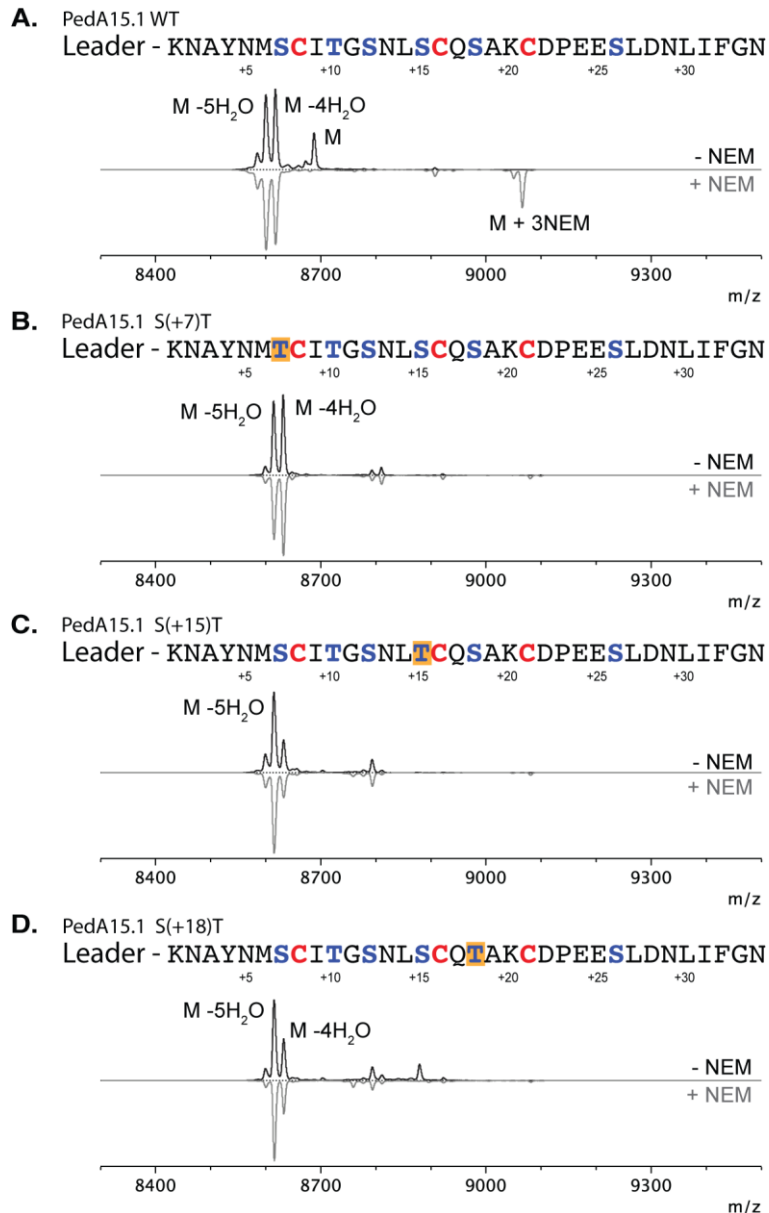


Figure S14: Ser-to-Thr His₆-PedA15.1 variants co-expressed with PedB15, PedC15, and *P. lusitanus* tRNA^{Glu}/GluRS in *E. coli*. Full-length purified peptides were analyzed by MALDI-TOF MS before (black) and after NEM alkylation (grey). (A) wild-type PedA15.1 contained a mixture of 4x dehydrated ([M+H] avg., m/z 8616.7 calc.; 8617.5 obs.) and 5x ([M+H] avg., m/z 8598.7 calc.; 8600.3 obs.) dehydrated product. (B) PedA15.1-S7T contained a mixture of 4x dehydrated ([M+H] avg., m/z 8630.7 calc.; 8631.7 obs.) and 5x ([M+H] avg., m/z 8612.7 calc.; 8614.4 obs.) dehydrated product. (C) PedA15.1-S15T contained predominantly 5x dehydrated ([M+H] avg., m/z 8612.7 calc.; 8614.9 obs.) product. (D) PedA15.1-S18T also contained predominantly 5x dehydrated ([M+H] avg., m/z 8612.7 calc.; 8614.7 obs.) product. All variants were fully cyclized as was evident by the lack of NEM adducts following NEM treatment. NEM, *N*-ethylmaleimide. Mutations are highlighted in orange.

PedA15.1 Trypsin: NAYNMS²CITG²SNL²SC²QSAK²CDPEESLDNLI²FGN

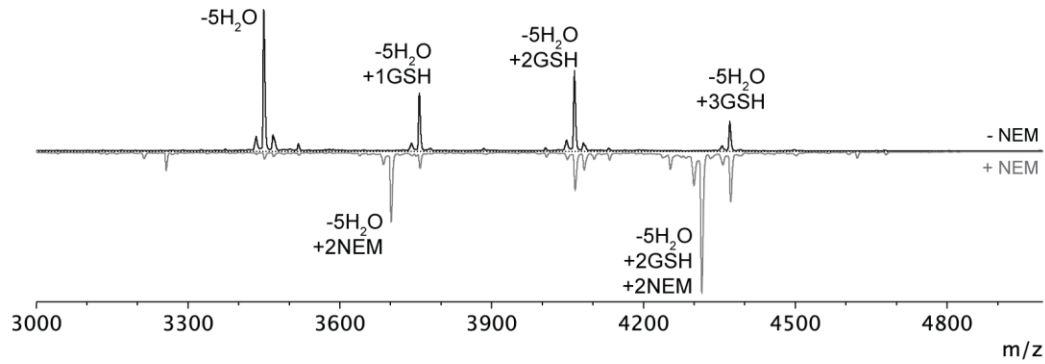


Figure S15: MALDI-TOF MS analysis of PedA15.1 expressed in the absence of PedC15 followed by trypsin digestion & NEM alkylation. Several glutathione (GSH) adducts are observed, as well as NEM adducts, indicating incomplete cyclization in the absence of PedC15. PedA15.1 – 5 H₂O (M, avg. m/z 3449.8 calc.; 3450.0.3 obs.), PedA15.1 – 5 H₂O + 2 NEM ([M+H], avg. m/z 3701.0 calc.; 3701.2 obs.), PedA15.1 – 5 H₂O + GSH ([M+H], avg. m/z 3758.1 calc.; 3758.4 obs.), PedA15.1 – 5 H₂O + 2 GSH ([M+H], avg. m/z 4064.4 calc.; 4064.8 obs.), PedA15.1 – 5 H₂O + 3 GSH ([M+H], avg. m/z 4372.8 calc.; 4372.3 obs. PedA15.1 – 5 H₂O + 2 GSH + 2NEM ([M+H], avg. m/z 4315.7 calc.; 4315.1 obs.).

PedA15.2 LahT150: GAHANNM**S**C**I**T**G****S**K**S**C**P**N**C**KEAEREDYN

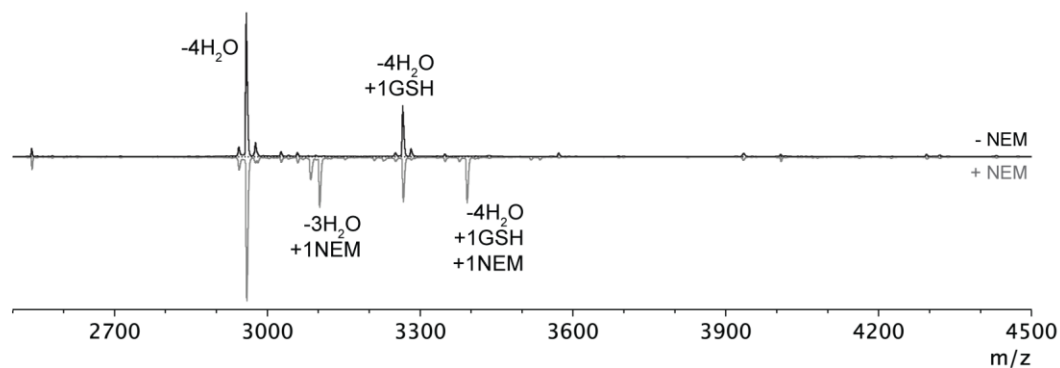


Figure S16: MALDI-TOF MS analysis of PedA15.2 expressed in the absence of PedC15 followed by LahT150 digestion & NEM alkylation. A glutathione (GSH) adduct is observed, as well as NEM adducts, indicating incomplete cyclization in the absence of PedC15. PedA15.2 – 4 H₂O ([M+H], avg. m/z 2959.2 calc.; 2959.6 obs.), PedA15.2 – 3 H₂O + NEM ([M+H], avg. m/z 3102.3 calc.; 3102.9 obs.), PedA15.2 – 4 H₂O + GSH ([M+H], avg. m/z 3266.5 calc.; 3266.2 obs.), PedA15.2 – 4 H₂O + 1 GSH +1 NEM ([M+H], avg. m/z 3391.6 calc.; 3392.1 obs.).

NisC	MGLAHGLAG _[207]RDAWCYGG _[287]YMICHGY _[333]FLEGI _[382]
WP_125426353.1	TGISHGSAM _[203]NLCLLYGD _[265]ASLWYGT _[315]FNFGV _[377]
WP_184623966.1	TGLSHGNGM _[206]NHCIIVYGD _[268]MSIKYGV _[318]FSFGL _[380]
WP_041881201.1	TGLAHGNGM _[207]NHCVVYGD _[268]ASVKYGV _[318]FGYGL _[380]
WP_184659139.1	TGLAHGNAM _[208]NHCVVYGD _[269]ASIKYGV _[319]FGYGL _[381]
WP_158797083.1	TGLAHGNAM _[201]NHCLVYGD _[266]ASVKYGA _[316]LNFGL _[378]
WP_154282285.1	TGLAHGSAM _[201]NHCLVYGD _[266]ASVKYGV _[316]LNFGL _[378]
WP_193419311.1	TGLAHGVAM _[201]NHCLVYGD _[266]ASVKYGV _[316]LNFGL _[378]
WP_147230291.1	TGLAHGSAM _[201]NHCLVYGD _[266]ASVKYGV _[316]LNFGL _[378]
WP_183766846.1	FGFPHGYLS _[201]NHCLVYGD _[266]DSVKYGV _[316]LNFGL _[378]
WP_100924802.1	FGFPHGYLS _[191]RLAWCNSD _[266]HHFCHGS _[312]LFY GK _[365]

Figure S17: Sequence alignment of lanthipeptide cyclases encoded in genomes of various Bacteroidetes. Sequence of cyclases obtained from the RODEO output that was used for generating Figure S13. Putative active site residues are highlighted based on previous structural and mutagenesis studies on the lantibiotic cyclase NisC:^{10, 11} non-essential (gray), catalytic acid (yellow), and zinc-binding (cyan) residues. Nearly all orthologs of PedC15 lack zinc-binding ligands (except WP_100924802.1).

References

- (1) Gibson, D. G., Young, L., Chuang, R. Y., Venter, J. C., Hutchison, C. A., 3rd, and Smith, H. O. (2009) Enzymatic assembly of DNA molecules up to several hundred kilobases, *Nat. Methods* 6, 343-345.
- (2) Caetano, T., Krawczyk, J. M., Mosker, E., Süßmuth, R. D., and Mendo, S. (2011) Heterologous expression, biosynthesis, and mutagenesis of type II lantibiotics from *Bacillus licheniformis* in *Escherichia coli*, *Chem. Biol.* 18, 90-100.
- (3) Bobeica, S. C., Dong, S. H., Huo, L., Mazo, N., McLaughlin, M. I., Jimenez-Oses, G., Nair, S. K., and van der Donk, W. A. (2019) Insights into AMS/PCAT transporters from biochemical and structural characterization of a double glycine motif protease, *eLife* 8, e42305.
- (4) Strohmalm, M., Hassman, M., Košata, B., and Kodíček, M. (2008) mMass data miner: an open source alternative for mass spectrometric data analysis, *Rapid Commun. Mass Spec.* 22, 905-908.
- (5) Thibodeaux, C. J., Ha, T., and van der Donk, W. A. (2014) A price to pay for relaxed substrate specificity: a comparative kinetic analysis of the class II lanthipeptide synthetases ProcM and HalM2, *J. Am. Chem. Soc.* 136, 17513-17529.
- (6) Liu, W., Chan, A. S. H., Liu, H., Cochrane, S. A., and Vederas, J. C. (2011) Solid supported chemical syntheses of both components of the lantibiotic lacticin 3147, *J. Am. Chem. Soc.* 133, 14216-14219.
- (7) Bobeica, S. C., Zhu, L., Acedo, J. Z., Tang, W., and van der Donk, W. A. (2020) Structural determinants of macrocyclization in substrate-controlled lanthipeptide biosynthetic pathways, *Chem. Sci.* 11, 12854-12870.
- (8) Altschul, S. F., Gish, W., Miller, W., Myers, E. W., and Lipman, D. J. (1990) Basic local alignment search tool, *J. Mol. Biol.* 215, 403-410.
- (9) Tietz, J. I., Schwalen, C. J., Patel, P. S., Maxson, T., Blair, P. M., Tai, H. C., Zakai, U. I., and Mitchell, D. A. (2017) A new genome-mining tool redefines the lasso peptide biosynthetic landscape, *Nat. Chem. Biol.* 13, 470-478.

- (10) Li, B., and van der Donk, W. A. (2007) Identification of essential catalytic residues of the cyclase NisC involved in the biosynthesis of nisin, *J. Biol. Chem.* *282*, 21169-21175.
- (11) Yang, X., and van der Donk, W. A. (2015) Michael-type cyclizations in lantibiotic biosynthesis are reversible, *ACS Chem. Biol.* *10*, 1234-1238.